The vibrating inhomogeneous string

George Rawitscher and Jakob Liss
Department of Physics, University of Connecticut, Storrs, Connecticut, 06269

(Received 24 February 2010; accepted 11 November 2010)

We solve the integral equation that describes an oscillating inhomogeneous string by using a spectral expansion method in terms of Chebyshev polynomials. The result is compared with the solution of the corresponding differential equation, obtained by an expansion into a set of sine-wave functions. The accuracy of the two methods is determined by comparison with an iterative method, which allows a precision of one part in 10^{11}. This iterative method is based on a method introduced by Hartree and is implemented by using the spectral expansion procedures. © *2011 American Association of Physics Teachers.*

[DOI: 10.1119/1.3534837]

I. INTRODUCTION

Excellent textbooks[1] are now available for courses in computational physics, as well as papers describing such courses.[2] The vibrating string provides an appealing topic for such courses[3] because the solution of the corresponding differential equation can be achieved in several ways, and comparisons of the different methods can be provided.

If the string is inhomogeneous, the separation of variables method becomes more complicated than for the homogenous case because the equation for the spatial part becomes a Sturm–Liouville eigenvalue equation whose solutions are no longer given by a simple set of sine waves. This Sturm-Liouville equation is usually solved by an expansion into a basis set of functions, which are the sine waves for a clamped homogeneous string, and which leads to a matrix equation for the expansion coefficients (this method will be denoted as the Fourier expansion method). The eigenvalues and eigenvectors of this matrix provide the Sturm–Liouville functions, and hence the accuracy depends on the size of the basis and hence on the size of the matrix.

Another method for solving the Sturm–Liouville differential equation consists of introducing an integral equation version of the Sturm–Liouville differential equation and solving the latter by an expansion into Chebyshev polynomials.[4,5] The advantage of this method, to be denoted as the integral equation method (IEM), is that its accuracy can be automatically pre-determined; the number of mesh points required to achieve a particular accuracy is much smaller than for finite difference methods,[5] and the size of the matrices is kept small by a partition technique, thus avoiding the limitations of large dense matrices in conventional integral equation solution methods.[6]

The purpose of this paper is to explain the integral equation method in simple terms, and to apply it to the solution of the inhomogeneous vibrating string. For comparison purposes a more conventional Fourier expansion method will be described in Sec. II. As preparation to the IEM the convergence properties of the expansion of a function into Chebyshev polynomials and the truncation errors of the expansion are described in Sec. III. The integral equation that is equivalent to the Sturm–Liouville differential equation is presented in Sec. IV, and the solution by means of the Integral Equation Method is described. That solution leads to a matrix equation, whose eigenvalues and eigenfunctions are approximations to the desired solution of the Sturm–Liouville equation. A comparison of the eigenvalues obtained in Sec. II and those obtained in Sec. IV leads to a better understanding of the Fourier Expansion and the Integral Equation methods. In Sec. V the eigenvalues of the integral Sturm–Liouville equation are obtained by an iterative method (to be denoted as extended Hartree method). This method avoids having to obtain the eigenvalues of a big matrix, which is the case with the two other methods described above, and whose accuracy is not *a priori* known, by finding each eigenvalue iteratively, with a precision that can be pre-determined. This method was first devised by Hartree[7] for the solution of energy eigenvalues of the Schrödinger equation, and has been adapted to the solution of the integral equation based on the expansion into Chebyshev polynomials.[8] We adapt this method to the solution of the vibrating inhomogeneous string. Because it can achieve an accuracy of one part in 10^{11} for both the eigenvalues and eigenfunctions of the Sturm–Liouville equation, it can provide benchmark values against which the results of other methods can be compared. Section VI summarizes our results and conclusions.

Expansions into Chebyshev polynomials converge quickly under certain conditions. Mathematicians use the word "spectral" to denote this convergence property; in this context, spectral does not imply the spectra of frequencies. The general method of spectral expansions is not new (since ca. 1970).[9] Its realization in terms of Chebyshev expansions as applied to the solution of the vibrating string Sturm–Liouville integral equation, described here in Secs. III and IV, is the main purpose of this paper. The method for the solution of the string equation is similar to the solution of the time independent Schrödinger equation. Because the properties of the string are much easier to visualize than the properties of the Schrödinger equation, the present discussion also serves as an introduction to several numerical methods for obtaining the eigenvalues and eigenfunctions of the Schrödinger equation. The numerical calculations are done with Matlab,[10] and the programs for the calculations we discuss are available in the Compadre digital library.[11]

II. THE INHOMOGENEOUS VIBRATING STRING

Consider a stretched metallic string clamped between two horizontal points The distance between the fixed points is L, and the mass per unit length ρ of the string is not a constant,[12,13] and hence the speed of propagation of the waves depends on the location along the string. When a dis-

turbance is imparted to the string, the particles in the string vibrate in the vertical direction with a distribution of frequencies that is to be determined.

We denote by $y(x,t)$ the (small) displacement of a point on the string in the vertical direction away from the equilibrium position $y=0$ at a horizontal distance x of the point from the left end at time t. The wave equation is

$$\frac{\partial^2 y}{\partial x^2} - \frac{\rho}{T}\frac{\partial^2 y}{\partial t^2} = 0, \tag{1}$$

where T is the tension along the string. We define the dimensionless function $\mathcal{R}(x)$ which describes the variation of ρ with x as

$$\rho(x) = \rho_0 \mathcal{R}(x), \tag{2}$$

where ρ_0 is some fixed value of ρ. If we define the reference speed c by $\rho_0/T = 1/c^2$, Eq. (1) becomes

$$\frac{\partial^2 y}{\partial x^2} - \frac{1}{c^2}\mathcal{R}(x)\frac{\partial^2 y}{\partial t^2} = 0. \tag{3}$$

If we use separation of variables, $y(x,t) = \psi(x)A(t)$, we obtain

$$\frac{d^2\psi(x)}{dx^2} + \Lambda \mathcal{R}(x)\psi(x) = 0, \tag{4}$$

and

$$\frac{d^2 A}{dt^2} = -\Lambda c^2 A. \tag{5}$$

A general solution of Eq. (5) is $a\cos(\omega t) + b\sin(\omega t)$, with $\omega = c\sqrt{\Lambda}$, where Λ is an eigenvalue of Eq. (4) that is assumed to be positive.

Equation (4) is a Sturm–Liouville equation[14] with an infinite set of eigenvalues Λ_n $(n=1,2,3,\ldots)$. The corresponding eigenfunctions $\psi_n(x)$ form a complete set in terms of which the general solution can be written as

$$y(x,t) = \sum_{n=1}^{\infty} [a_n \cos(\omega_n t) + b_n \sin(\omega_n t)]\psi_n(x), \tag{6}$$

where $w_n = c\sqrt{\Lambda_n}$. The objective is to calculate the functions $\psi_n(x)$ and the eigenvalues Λ_n as solutions of Eq. (4), with the boundary conditions that $y=0$ both for $x=0$ and $x=L$,

$$\psi_n(0) = \psi_n(L) = 0, \tag{7}$$

and for $t=0$

$$y(x,0) = f(x) \quad \text{and} \quad dy/dt|_{t=0} = g(x). \tag{8}$$

The constants a_n and b_n in Eq. (6) are obtained from the initial displacement of the string from its equilibrium position $f(x)$ and the initial velocity $g(x)$ in terms of integrals of the functions $\psi_n(x)$.

$$a_n = \int_0^L f(x)\psi_n(x)dx, \quad b_n = \frac{1}{\omega_n}\int_0^L g(x)\psi_n(x)dx. \tag{9}$$

A. The homogeneous string

If the string is homogeneous, $\mathcal{R}(x)=1$ and the ψ_n are given by sine functions. That is, $\psi_n(x) \equiv \phi_n(x)$, with

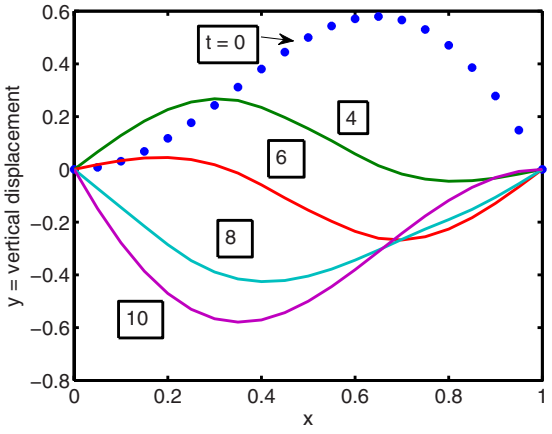

Fig. 1. Vibrations on the homogeneous string. The filled circles mark the initial displacement of the string from its equilibrium position, given by Eq. (11). The numbers next to each curve indicate the time in units of L/c.

$$\phi_n(x) = \sqrt{2/L}\,\sin(k_n x), \quad k_n = n(\pi/L) \quad (n=1,2,3\ldots), \tag{10}$$

and the eigenvalues become $\Lambda_n = k_n^2 = [n\pi/L]^2$. If we assume that the functions $f(x)$ and $g(x)$ are given by

$$f(x) = x\,\sin(\pi x/L), \quad g(x) = 0, \tag{11}$$

we can evaluate Eq. (9) for the coefficients a_n (all the $b_n = 0$). We find that all a_n vanish for n odd, with the exception of $n=1$, for which

$$a_1 = -\frac{L^2}{4}\sqrt{\frac{2}{L}}. \tag{12}$$

For n even, the result for a_n is

$$a_n = \frac{L^2}{\pi^2}\sqrt{\frac{2}{L}}\left[\frac{1}{(1+n)^2} - \frac{1}{(1-n)^2}\right] \quad (n=2,4,\ldots). \tag{13}$$

These results allow us to calculate the truncated form of the sum in Eq. (6)

$$y^{(n_{\max})}(x,t) = \sum_{n=1}^{n_{\max}} [a_n \cos(\omega_n t) + b_n \sin(\omega_n t)]\phi_n(x). \tag{14}$$

Some results are displayed in Fig. 1, using the values $L = 1$ m, $c = 800$ m/s, and with f and g given by Eq. (11). As time progresses, the wave reflects from the right clamping point, and after approximately 18 time units L/c, returns to its initial configuration.

For $n \gg 1$, a_n approaches 0 as $(1/n)^3$. It is desirable to examine how many terms are needed in the sum in Eq. (14) to obtain an accuracy of four significant figures in y. A good guess is that the sum of all terms not included in the sum

$$\sum_{n_{\max}+1}^{\infty} a_n \cos(\omega_n t) \simeq -4\frac{L^2}{\pi^2}\sqrt{\frac{2}{L}}\int_{n_{\max}+1}^{\infty}\frac{1}{n^3}\cos\left(\frac{c\pi}{L}tn\right)dn, \tag{15}$$

should be less than 10^{-4}. The integral in Eq. (15) is smaller than $\int_{n_{\max}+1}^{\infty}(1/n)^3 dn = (n_{\max}+1)^{-2}/2$ (because the cosine term produces cancellations), and we obtain the estimate

$$\left| \sum_{n_{\max}+1}^{\infty} a_n \cos(\omega_n t) \right| < 2\frac{L^2}{\pi^2}\sqrt{\frac{2}{L}}(n_{\max}+1)^{-2}. \tag{16}$$

For $n_{\max}=50$ the right-hand side of Eq. (16) is $\simeq 10^{-4}$. A numerical evaluation of the difference $|y^{(50)}(x,0)-f(x)|$, where $f(x)$ is defined in Eq. (11), is less than 10^{-5}, which confirms that for $n_{\max}=50$ the accuracy expected for $y^{(50)}\times(x,t)$ is better than one part in 10^4.

B. The solution of the inhomogeneous string by a Fourier series expansion

An approximate solution to Eq. (4) for ψ_n is to expand it in terms of the sine functions in Eq. (10) because these functions obey the same boundary conditions as ψ_n. The approximation consists in truncating this expansion at the upper limit $\ell_{\max}=N$. We drop the subscript and superscript (n) for now, and write

$$\psi^{(N)}(x) = \sum_{\ell'=1}^{N} d_{\ell'}\phi_{\ell'}(x). \tag{17}$$

We substitute Eq. (17) into Eq. (4), remember that $d^2\phi_\ell(x)/dt^2=-k_\ell^2\phi_\ell(x)$, multiply Eq. (4) by the function $\phi_\ell(x)$, integrate both sides of the equation over dx from $x=0$ to $x=L$, and use the orthonormality of the functions $\phi_\ell(x)$ to obtain

$$-k_\ell^2 d_\ell + \Lambda \sum_{\ell'=1}^{N} R_{\ell,\ell'} d_{\ell'} = 0, \tag{18}$$

where

$$R_{\ell,\ell'} = \int_0^L \phi_\ell(x)\mathcal{R}(x)\phi_{\ell'}(x)dx \tag{19}$$

are the matrix elements of the function $\mathcal{R}$ over the basis functions ϕ_ℓ. Equation (18) can also be written in the matrix form

$$\begin{pmatrix} k_1^2 & & & & \\ & k_2^2 & & & \\ & & k_3^2 & & \\ & & & \ddots & \\ & & & & k_N^2 \end{pmatrix} \begin{pmatrix} d_1 \\ d_2 \\ d_3 \\ \vdots \\ d_N \end{pmatrix} = \Lambda \begin{pmatrix} R_{1,1} & R_{1,2} & R_{1,3} & \cdots & R_{1,N} \\ R_{2,1} & R_{2,2} & R_{2,3} & \cdots & R_{2,N} \\ R_{3,1} & R_{3,2} & R_{3,3} & \cdots & R_{3,N} \\ \vdots & \vdots & \vdots & \ddots & \vdots \\ R_{N,1} & R_{N,2} & R_{N,3} & \cdots & R_{N,N} \end{pmatrix} \begin{pmatrix} d_1 \\ d_2 \\ d_3 \\ \vdots \\ d_N \end{pmatrix}, \tag{20}$$

or more succinctly as

$$\mathbf{k}^2\vec{d} = \Lambda \mathbf{R}\vec{d}. \tag{21}$$

Bold letters indicate matrices, and a vector quantity indicates a $(N\times 1)$ column. Because all the k_ℓ are positive, the matrix $\mathbf{k}^{-1}$ can be defined as

$$\mathbf{k}^{-1} = \begin{pmatrix} k_1^{-1} & & & & \\ & k_2^{-1} & & & \\ & & k_3^{-1} & & \\ & & & \ddots & \\ & & & & k_N^{-1} \end{pmatrix}, \tag{22}$$

and we can transform Eq. (21) to

$$\mathbf{M}_{\text{fourier}}\vec{u}_n = \frac{1}{\Lambda_s}\vec{u}_n, \quad (n=1,2,\ldots N), \tag{23}$$

where

$$\mathbf{M}_{\text{fourier}} = \mathbf{k}^{-1}\mathbf{R}\mathbf{k}^{-1}, \tag{24}$$

and

$$\vec{u}_n = \mathbf{k}\vec{d}_n. \tag{25}$$

Although Eq. (21) is a generalized eigenvalue equation, Eq. (23) is a simple eigenvalue equation. The vectors $\vec{u}_n$ are the N eigenvectors of the $N\times N$ matrix $\mathbf{M}_{\text{fourier}}$, and $1/\Lambda_n$ are the eigenvalues. Because $\mathbf{R}$ is a symmetric matrix, $\mathbf{M}_{\text{fourier}}$ is also symmetric. The eigenvectors of a symmetric matrix are orthogonal to each other, that is, $(\vec{u}_n)^T\cdot\vec{u}_m=\delta_{n,m}$. Here T indicates transposition. However, the vectors $\vec{d}_n$ are not orthogonal to each other because $(\vec{d}_n)^T\cdot\vec{d}_m=(\vec{u}_n)^T\mathbf{k}^{-2}\vec{u}_m$.

In summary, the procedure for obtaining the solution of the inhomogeneous string by a Fourier series expansion is as follows:

1. Choose an upper truncation limit N of the sum (17).
2. Calculate the matrix elements $R_{\ell,\ell'}$ to obtain the $N\times N$ matrix $\mathbf{R}$.
3. Construct the matrix $\mathbf{M}_{\text{fourier}}$ from Eq. (24), and find the eigenvalues $1/\Lambda_n$ and eigenvectors $\vec{u}_n$, $(n=1,2,\ldots,N)$, by using the Matlab eigenvalue command $[\mathbf{V},\mathbf{D}]=\text{eig}(\mathbf{M})$. The output $\mathbf{D}$ is a diagonal matrix of the eigenvalues, and $\mathbf{V}$ is a matrix whose columns are the corresponding eigenvectors, so that $\mathbf{MV}=\mathbf{VD}$.
4. Let $\vec{\Phi}(x)$ be the column vector of the N basis functions $\phi_\ell(x)$. Then $\psi(x)$ can be written as (the superscript N is dropped)
$$\psi_n(x) = (\vec{u}_n)^T\mathbf{k}^{-1}\cdot\vec{\Phi}(x). \tag{26}$$
5. From Eq. (26) the coefficients a_n and b_n can be written as
$$a_n = \langle f\psi_n\rangle = (\vec{u}_n)^T\mathbf{k}^{-1}\cdot\langle f\vec{\Phi}(x)\rangle \tag{27a}$$
$$b_n = \langle g\psi_n\rangle = (\vec{u}_n)^T\mathbf{k}^{-1}\cdot\langle g\vec{\Phi}(x)\rangle, \tag{27b}$$
where $\langle f\vec{\Phi}(x)\rangle$ is the column vector of the integrals $\langle f\phi_\ell\rangle=\int_0^L f(x)\phi_\ell(x)dx$, $(\ell=1,2,\ldots,N)$.
6. The final expression for $y(x,t)$ can be obtained by first obtaining the coefficients e_n
$$e_n(t) = (\vec{u}_n)^T\mathbf{k}^{-1}\left[\langle f\vec{\Phi}(x)\rangle\cos(w_n t) + \langle g\vec{\Phi}(x)\rangle\frac{1}{w_n}\sin(w_n t)\right], \tag{28}$$
and then performing the sum

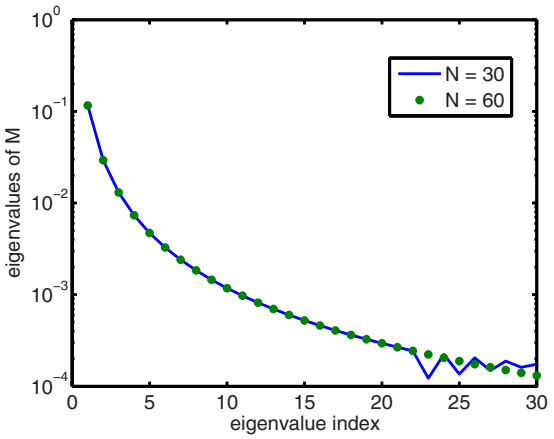

Fig. 2. The eigenvalues of the matrix $\mathbf{M}_{\text{fourier}}$ defined in Eq. (24). The quantity N indicates the truncation value of the sum in Eq. (17). The dimension of the matrix $\mathbf{M}_{\text{fourier}}$ is $N\times N$. The figure shows that the eigenvalues of an $N\times N$ matrix become unreliable for an eigenvalue index close to N.

$$y(x,t)=\sum_{n=1}^{N} e_n(t)\psi_n(x)=\vec{e}^{\,T}\cdot\vec{\Psi}, \tag{29}$$

where $\vec{e}$ is the column vector of e_n, and $\vec{\Psi}$ is the column vector of ψ_n. We limit ourselves in this paper to calculating the eigenvalues Λ_n and to studying their accuracy.

We assume that $\mathcal{R}(x)$ changes with the distance x from the left end of the string as

$$\mathcal{R}(x)=1+2x^2, \tag{30}$$

The integrals (19) for the matrix elements $R_{\ell,\ell'}$ can be obtained analytically with the result

$$R_{\ell,\ell'}=4\left(\frac{L}{\pi}\right)^2(-1)^{\ell+\ell'}\left[\frac{1}{(\ell-\ell')^2}-\frac{1}{(\ell+\ell')^2}\right]\quad(\ell\neq\ell') \tag{31}$$

$$R_{\ell,\ell}=1+2L^2\left[\frac{1}{3}-\frac{2}{(2\pi\ell)^2}\right]\quad(\ell=\ell'). \tag{32}$$

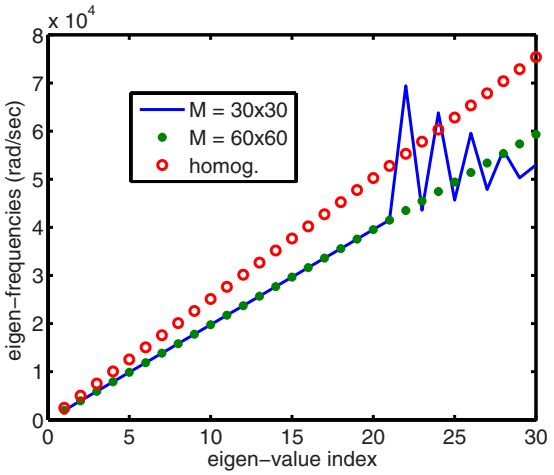

Fig. 3. The frequencies in units of rad/s of the vibrations of the inhomogeneous string, compared with the frequencies of the corresponding homogeneous string. The higher frequencies become inaccurate when the dimension of the matrix $\mathbf{M}_{\text{fourier}}$ is too small.

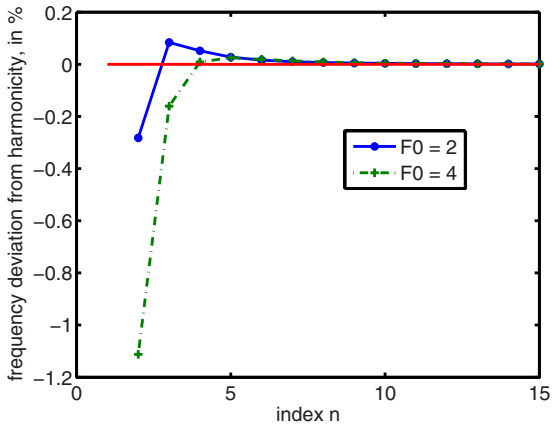

Fig. 4. The deviation from harmonicity as a function of the eigenfrequency index n for two inhomogeneities. The deviation is defined in terms of the difference between two neighboring frequencies $d(n)=[\omega(n)-\omega(n-1)]$ as $100\{d(n+1)/d(n)-1\}$. The inhomogeneity is given by $R(x)=1+F_0x^2$ with F_0 either 2 or 4.

The numerical determination of the matrices $\mathbf{R}$ and $\mathbf{M}_{\text{fourier}}$, using the same numerical values for L and c as for the homogeneous string, is accomplished with the program string_fourier which calls the function inh_str_M, both of which are written in Matlab by the authors. The value of N in the sum (17) is set equal to either 30 or 60, and the corresponding dimension of the matrices $\mathbf{M}_{\text{fourier}}$ and $\mathbf{R}$ are $N\times N$.

The results for the eigenvalues Λ_n are shown in Fig. 2 and the corresponding frequencies are shown in Fig. 3. The frequencies for $\mathcal{R}(x)=1$ are given by the open circles in Fig. 3. Because the inhomogeneous string is more dense at large values of x than the homogeneous one, the corresponding eigenfrequencies are correspondingly smaller. The eigenfrequencies of the inhomogeneous string nearly fall on a straight line, which means that the frequencies are nearly equispaced; that is, they nearly follow the same harmonic relation as the ones for the homogeneous string. The reason for this property has not been investigated, but could be related to the possibility of mapping the spectrum of an inhomogeneous string to that of a homogeneous one.[12] Near the fundamental frequency slight deviations from harmonicity occur, as illustrated in Fig. 4. However, small deviations from harmonicity are also caused by other effects such as the stiffness of the string.

Figures 2 and 3 show that for $N=30$, the eigenvalues become unreliable for $n\geq 22$. This discrepancy is a general property of the high-n eigenvalues of a finite non-diagonal matrix. Table I and Fig. 5 illustrate the dependence of the eigenvalues on N by comparing two eigenvalues for the same n of the matrix $\mathbf{M}_{\text{fourier}}$ for $N=30$ and $N=60$. The iterative method described in Sec. V does not suffer from this inaccuracy.

Table I. Eigenvalues of the matrix $\mathbf{M}$, Eq. (24) for two different dimensions.

n	N=30	N=60
1	$1.614775590198150\times10^{-1}$	$1.6147755902115\times10^{-1}$
20	4.092×10^{-4}	$4.0933853097811\times10^{-4}$

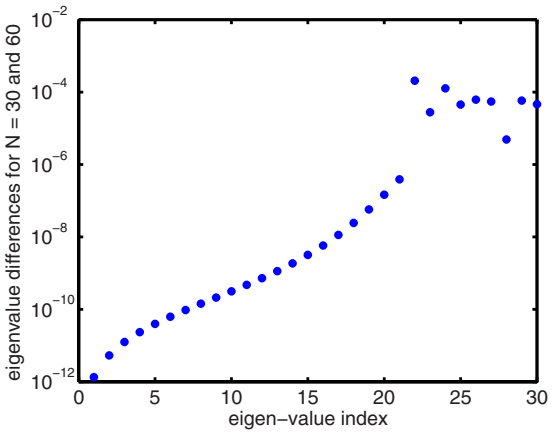

Fig. 5. The dependence of the eigenvalues of the matrix $\mathbf{M}_{\text{fourier}}$ on the dimension $N\times N$ of the matrix. The y-axis shows the absolute value of the difference between two sets of eigenvalues, one for $N=30$, the other for $N=60$. Some numerical values are given in Table I. The figure and Table I table illustrate the sensitivity of the eigenvalue to the matrix truncation number N.

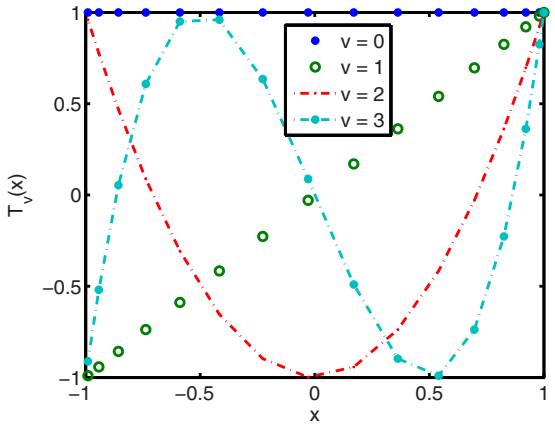

Fig. 6. Chebyshev polynomials for indices $v=0$, 1, 2, and 3. They are calculated from $T_v(x)=\cos(v\theta)$ for equispaced angles θ, which shows that the corresponding points in x are not equispaced.

III. SPECTRAL EXPANSIONS INTO CHEBYSHEV POLYNOMIALS

We first describe some of the properties of Chebyshev polynomials, and then present the Curtis–Clenshaw method[15] for expanding functions in terms of the Chebyshev polynomials, with an emphasis on the errors associated with the truncation of the expansion. The motivation is to make meaningful the application of these expansions to solving integral equations, which is basically the IEM.

A. Properties of Chebyshev polynomials

The Chebyshev polynomials $T_n(x)$ $n=0,1,2,\ldots$ provide a useful set of basis functions.[16,17] We review the properties needed for the present application in the following. The variable x is in the interval $[-1,+1]$, and is related to the angle θ by $x=\cos\theta$. In terms of x the T_n are given by $T_0=1$, $T_1=x$, $T_2=2x^2-1$, and $T_{n+1}=2xT_n-T_{n-1}$. In terms of θ they are

$$T_n=\cos(n\theta) \quad (0\le\theta\le\pi). \tag{33}$$

It is clear from Eq. (33) that $-1\le T_n(x)\le 1$, and the larger n, the more zeros these polynomials have. The T_n are orthogonal to each other with the weight function $(1-x^2)^{-1/2}$. The integral

$$\int_{-1}^{+1} T_n(x)T_m(x)(1-x^2)^{-1/2}dx=\int_0^{\pi}\cos(n\theta)\cos(m\theta)d\theta, \tag{34}$$

is 0 if $n\neq m$, $\pi/2$ if $n=m\neq 0$, and π if $n=m=0$. A plot of $T_n(x)$ for $n=0$, 1, 2, and 3 is shown in Fig. 6, (where the subscript n is denoted as v) which illustrates that for equispaced values of θ the corresponding values of x are not equispaced.

The values of x, denoted as ξ_i, for which $T_n=0$, are also not equispaced. As can be seen from Eq. (33) the zeros ξ_i of $T_{N+1}(x)$ are given for $N\ge 0$ by

$$\xi_i=\cos\left[\frac{(2i+1)}{2N+2}\pi\right] \quad (i=0,1,2,\ldots N). \tag{35}$$

B. The expansion method

Consider a general function $f(r)$ defined in the interval $[a,b]$, not to be confused with the function defined in Eq. (11). To expand it into Chebyshev polynomials, we first transform the variable r to a new variable x defined in the interval $[-1,+1]$. This transformation can be achieved by the linear map

$$r=\alpha x+\beta, \tag{36}$$

with $\alpha=(b-a)/2$ and $\beta=(b+a)/2$. In terms of x we obtain the function $\bar{f}(x)=f(r)$, and the desired (truncated) expansion is

$$\bar{f}^{(N)}(x)=\sum_{n=0}^{N} a_nT_n(x). \tag{37}$$

The conventional method of obtaining the expansion coefficients a_n is to multiply Eq. (37) on both sides by $T_m(x)/\sqrt{1-x^2}$, integrate over x from -1 to $+1$, and use the orthogonality condition (34). A more computer friendly alternative was given in Ref. 15 and consists in writing Eq. (37) $N+1$ times for the zeros $\xi_0,\xi_1,\ldots,\xi_N$ of the first Chebyshev polynomial T_{N+1} not included in the sum (37). We thus obtain $N+1$ linear equations for the $N+1$ coefficients,

$$\bar{f}^{(N)}(\xi_0)=\sum_{n=0}^{N} a_nT_n(\xi_0) \tag{38a}$$

$$\bar{f}^{(N)}(\xi_1)=\sum_{n=0}^{N} a_nT_n(\xi_1) \tag{38b}$$

$$\vdots$$

$$\bar{f}^{(N)}(\xi_N)=\sum_{n=0}^{N} a_nT_n(\xi_N), \tag{38c}$$

which in matrix notation has the form

$$\begin{pmatrix} \bar{f}(\xi_0) \\ \bar{f}(\xi_1) \\ \vdots \\ \bar{f}(\xi_N) \end{pmatrix} = C \begin{pmatrix} a_0 \\ a_1 \\ \vdots \\ a_n \end{pmatrix} \tag{39}$$

where C is known as the discrete cosine transform.[9] The points ξ_i are "support points" because the function $\bar{f}$ has to be known only at these points. The elements of the matrix C are $C_{i,j}=T_j(\xi_i)$, and its columns are orthogonal to each other. After column normalization, we obtain an orthogonal matrix, and hence the inverse C^{-1} can be easily obtained, without the need to invoke a numerical matrix inversion algorithm. The matrix C^{-1} is denoted as CM1 in the Matlab function [C,CM1,z]=C_CM1(N).[11] The row vector z contains the values ξ_i in descending order $(i=N,N-1,\ldots,0)$. If we insert the values of a_i obtained from Eq. (39) into Eq. (37), we obtain the value of the truncated function $\bar{f}^{(N)}(x)$ at any point in the interval $[-1,+1]$, and hence the procedure is also an interpolation method.[18,19]

How good is the approximation (37) to $\bar{f}(x)$? If the function is differentiable p times, it can be shown that

$$|\bar{f}^{(N)}(x)-\bar{f}(x)| \le \frac{K}{p-1}\frac{1}{N^{p-1}}, \tag{40}$$

where the constant K depends on the pth derivative of $\bar{f}$. If the function $\bar{f}$ is infinitely differentiable, then $p=\infty$ and the error in Eq. (40) decreases with N faster than any power of N. This decrease is known as the supra-algebraic convergence of the approximation of $\bar{f}^{(N)}(x)$ to $\bar{f}(x)$, a property also denoted by the term "spectral."[9] The expansion of $\bar{f}(x)$ in terms of Chebyshev polynomials[18,19] displays a spectral convergence in addition to converging uniformly.[19]

According to Theorem 2 in Ref. 17 the deviation of $\bar{f}^{(N)}(x)$ from $\bar{f}(x)$ is given by

$$|\bar{f}^{(N)}(x)-\bar{f}(x)| \simeq a_{N+1}T_{N+1}(x)[1+2xa_{N+2}/a_{N+1}], \tag{41}$$

which in practice can be rewritten as

$$|\bar{f}^{(N)}(x)-\bar{f}(x)| \le |a_{N+1}|. \tag{42}$$

Equations (41) and (42) can be understood from the fact that once N is sufficiently large, then for spectral expansions the values of a_n for $n>N$ decrease very rapidly to zero, and because the T_n have a magnitude less than 1, the residual sum in Eq. (37) is less than or equal to a_{N+1}. Equation (42) enables us to pre-assign an accuracy requirement tol for the expansion (37). For a given value of N, the size of one or of several of the partitions of the domain of r from 0 to $r_{\max}$ within which the function $f(r)$ is expanded can be determined adaptively, or else, for a given size of the partitions, a value of N can be determined for each partition such that in either case the sum of the absolute values of the last three expansion coefficients a_{N-2}, a_{N-1}, and a_N is less than the value of tol.

We now give an example that shows that, if the function f is not infinitely differentiable, then the corresponding Chebyshev expansion converges slowly. The two functions to be expanded are

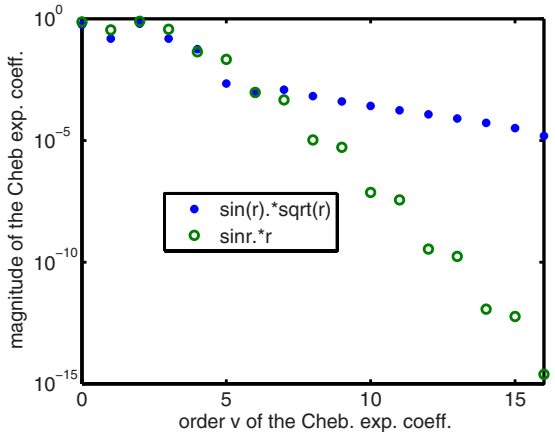

Fig. 7. The Chebyshev expansion coefficients as a function of the index v for the functions f_1 and f_2, defined in Eq. (42). Because the derivatives of f_1 have a singularity at the origin, the Chebyshev expansion converges more slowly than that of f_2, which has an infinite number of non-singular derivatives.

$$f_1(r) = r^{1/2}\sin(r) \tag{43a}$$

$$f_2(r) = r\sin(r) \tag{43b}$$

in the interval $0\le r\le\pi$. Although f_2 is infinitely differentiable, all the derivatives of f_1 are singular at $r=0$. The results for the Chebyshev expansions for f_1 and f_2 using the Curtis–Clenshaw method[15] are displayed in Fig. 7.

An expansion in a Fourier series of the function $f(r)=r\sin(\pi r)$ for $0\le r\le 1$ is also done for comparison with the Chebyshev expansion. We find that, with the exception of $n=1$, all Fourier coefficients a_n defined in Eqs. (9)–(13) vanish for odd n. For $n\gg 1$, a_n approaches 0 as $-4\sqrt{(2/\pi)}\times(1/n)^3$. The absolute value of a_n is shown in Fig. 8. In comparison to Fig. 7 we see that the Fourier expansion coefficients decrease with n more slowly than the Chebyshev expansion coefficients.

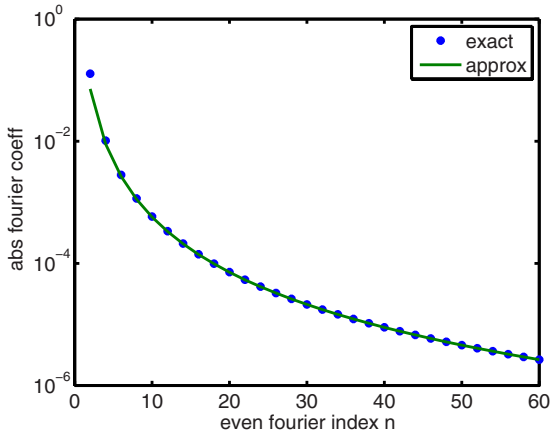

Fig. 8. The Fourier expansion coefficients of the function $f(x)=x\sin(\pi x)$ in the interval $[0,1]$ in terms of the basis functions $\sqrt{\pi}\sin(n\pi x)$. The analytic result, given by Eqs. (12) and (13) with $L=1$, is given by the filled circles. For odd values of $n\neq 1$ they are zero. The solid line represents an approximation to $|a_n|\simeq 4\sqrt{(2/\pi)}(1/n)^3$.

C. Integrals based on spectral expansions

To prepare for representing an integral operator in terms of Chebyshev polynomials, the integrals of Chebyshev expansions will now be discussed.[20] Given a function $f(r)$ defined in the interval $a \le r \le b$, we will obtain an approximation to the indefinite integral $I(r)$

$$I(r) = \int_a^r f(r')dr'. \tag{44}$$

As is done in Eq. (36) the function $f(r)$ is transformed to the function $\bar{f}(x)$ for the variable $x \subset [-1,+1]$. Then the integral (44) becomes

$$I(r) = \frac{(b-a)}{2} I_L(x), \tag{45}$$

where

$$I_L(x) = \int_{-1}^{x} \bar{f}(x')dx'. \tag{46}$$

We wish to obtain the convergence property of the approximation to $I_L(x)$

$$I_L^{(N)}(x) = \sum_{n=0}^{N} b_n T_n(x), \tag{47}$$

where it is assumed that $\bar{f}(x)$ has been expanded in a series of Chebyshev polynomials, as given by Eq. (37). In view of the integral properties of Chebyshev polynomials, the coefficients b_n can be expressed in terms of the expansion coefficients a_n of $\bar{f}(x)$,

$$\begin{pmatrix} b_0 \\ b_1 \\ \vdots \\ b_N \end{pmatrix} = S_L \begin{pmatrix} a_0 \\ a_1 \\ \vdots \\ a_N \end{pmatrix} \tag{48}$$

by means of the matrix S_L (Ref. 15) without loss of accuracy. For the integral

$$I_R(x) = \int_x^1 \bar{f}(x')dx' \tag{49}$$

an expression similar to that in Eq. (48) exists, with the matrix S_L replaced by S_R. Numerical expressions for the matrices S_L and S_R can be found in Refs. 4 and 11 under the name SL_SR. In particular, by noting that $T_n(1)=1$ for all n, an approximation to the definite integral $I(r_2)=\int_a^b f(r')dr'$ is given by

$$I^{(N)}(b) = \frac{(a-b)}{2} \sum_{n=0}^{N} b_n, \tag{50}$$

with an error comparable to Eq. (42) of the order of $|b_{N+1}|$. The method of evaluating a definite integral by means of Eq. (50) is denoted as Gauss–Chebyshev quadrature. The existence of Eq. (48) makes the expansion into Chebyshev polynomials suitable for the numerical solution of integral equations.

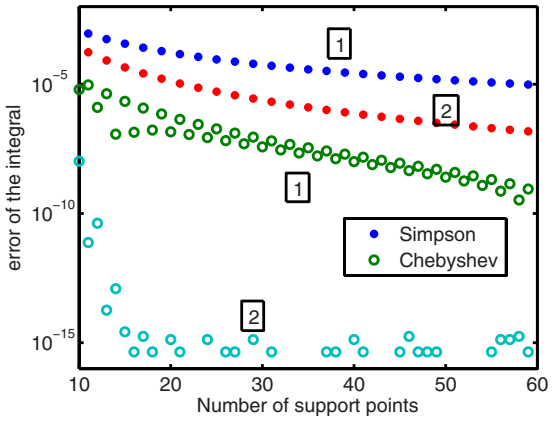

Fig. 9. Comparison of the convergence properties of the Gauss-Chebyshev and the Simpson integration procedures as a function of the number of support points. The labels 1 and 2 denote the integrals I_1 and I_2, defined in Eqs. (51a) and (51b), respectively. The figure illustrates that the integral of a singular function requires more meshpoints for its evaluation than a non-singular function to reach a given accuracy. Although the Chebyshev expansion method exhibits the same feature, it converges faster than the Simpson method. The latter is especially pronounced for the non-singular function.

As an example, the integrals

$$I_1 = \int_0^{\pi} r^{1/2} \sin(r)dr \tag{51a}$$

$$I_2 = \int_0^{\pi} r \sin(r)dr \tag{51b}$$

are evaluated using Eq. (50). For comparison purposes I_1 was also evaluated using the Matlab quadrature function quad(@myfun,0, π,acc), which calculates the integral by an adaptive finite difference method, where acc denotes the precision with which the quadrature result is given. The result is shown in the last line of Table II and demonstrates that the Gauss–Chebyshev quadrature method converges very slowly with N for discontinuous functions,[20] as a result of the slowness of the expansion of discontinuous functions, such as f_1, into Chebyshev polynomials.

For the analytic function $f_2(r)=r\sin(r)$ the corresponding integral converges with N much faster, reaching machine accuracy for $N=18$. These convergence properties are displayed in Fig. 9, where a comparison of the convergence using Simpson's quadrature method is also shown. It can be seen from Fig. 9 that the Simpson quadrature method converges faster for I_2 than I_1, but the Gauss–Chebyshev quadrature method converges even faster.

Table II. The results of the integral in Eq. (51a) obtained with the Chebyshev method. For this case the Chebyshev method with close to 60 expansion coefficients is accurate to only seven significant figures.

Chebyshev, $N=58$	2.43532116647
Chebyshev, $N=59$	2.43532116702
Quad, acc$=10^{-11}$	2.43532116417

IV. THE INTEGRAL EQUATION FOR THE INHOMOGENEOUS STRING

In Sec. II B the Sturm–Liouville functions $\psi_n(r)$, which are solutions of Eq. (4), were obtained by expanding them into a set of Fourier functions $\phi_\ell(r)$ and obtaining the eigenfunctions and eigenvalues of the resulting matrix $\mathbf{M}_{\text{fourier}}$. This matrix consists of overlap integrals of the function $\mathcal{R}(x)$ with the basis functions $\phi_\ell(x)$. In the present section we transform Eq. (4) into an integral equation because the numerical solution of the latter is more stable, that is, the roundoff errors accumulate more slowly, than for that of the former. We also avoid the need to do overlap integrals Eq. (19), to obtain the expansion coefficients. The basis functions are the Chebyshev polynomials for which the expansion series converges much faster than for the Fourier expansion. The use of integral equations to replace a Sturm–Liouville differential equation has been described in Ref. 13, and in the present application the integral equation will be solved numerically.

The integral equation that is equivalent to the Eq. (4) is

$$\frac{1}{\Lambda}\psi(r) = -\int_0^L \mathcal{G}(r,r')\mathcal{R}(r')\psi(r')dr', \tag{52}$$

where the Green's function $\mathcal{G}(r,r')$ is given by

$$\mathcal{G}(r,r') = \begin{cases} -\dfrac{1}{L}F(r)G(r') & (r<r') \\ -\dfrac{1}{L}F(r')G(r) & (r>r'), \end{cases} \tag{53}$$

and $F(r)=r$ and $G(r)=(L-r)$. Both F and G satisfy $d^2F/dr^2=0$ and $d^2G/dr^2=0$, and are linearly independent of each other. Because of the separable nature of $\mathcal{G}$, the integral on the right-hand side of Eq. (52) can be written as

$$\begin{aligned}\int_0^L \mathcal{G}(r,r')\mathcal{R}(r')\psi(r')dr' &= -\frac{1}{L}G(r)\int_0^r F(r')\mathcal{R}(r')\psi(r')dr' \\ &\quad -\frac{1}{L}F(r)\int_r^L G(r')\mathcal{R}(r')\psi(r')dr'. \end{aligned}\tag{54}$$

Because F vanishes at $r=0$ and G vanishes at $r=L$, and $\int_0^L \mathcal{G}(r,r')\mathcal{R}(r')\psi(r')dr'$ vanishes for both $r=0$ and $r=L$, the function ψ satisfies the boundary conditions and vanishes at both $x=0$ and $x=L$. These properties can be seen by setting the value of r in Eq. (54) equal to 0 and L, respectively. A proof that $\psi(r)$ defined by Eq. (52) satisfies Eq. (4) can be obtained by calculating the second derivative with respect to r of Eq. (54).

The numerical solution of Eq. (52) is accomplished by first changing the variable r, defined in the interval $[0,L]$, to the variable x, defined in the interval $[-1,+1]$, which results in the transformed functions $\bar{\psi}(x)$, $\bar{\mathcal{G}}(x,x')$, and $\bar{\mathcal{R}}(x')$. We expand the unknown solution $\bar{\psi}(x)$ in Chebyshev polynomials

$$\bar{\psi}(x) = \sum_{n=0}^{N} a_n T_n(x), \tag{55}$$

as was done in Eq. (37). Equation (52) leads to a matrix equation in the coefficients a_n, as we will now show. The coefficients a_n can be written as a column vector

$$\vec{a} = [a_0, a_1, \ldots, a_N]^T. \tag{56}$$

The values of $\bar{\psi}(\xi_i)$ at the support points ξ_i, which are the zeros of T_{N+1}, can also be expressed as a column vector

$$\vec{\psi} = [\bar{\psi}(\xi_0), \bar{\psi}(\xi_1), \ldots \bar{\psi}(\xi_N)]^T, \tag{57}$$

where the superscript T means transpose, and the relation between $\vec{a}$ and $\vec{\psi}$ given in Eq. (39) is

$$\vec{a} = \mathbf{C}^{-1}\vec{\psi}, \quad \vec{\psi} = \mathbf{C}\vec{a}. \tag{58}$$

Another important relation concerns the integrals

$$\Phi_L(x) = \int_{-1}^{x} \phi(x')dx' \quad \text{and} \quad \Phi_R(x) = \int_{x}^{1} \phi(x')dx', \tag{59}$$

where the general function ϕ is defined in the interval $[-1,1]$, and the corresponding expansion coefficients α_n are given by $\vec{\alpha}=\mathbf{C}^{-1}\vec{\phi}$. If $\Phi_L(x)$ and $\Phi_R(x)$ are expanded in Chebyshev polynomials

$$\Phi_L(x) = \sum_{n=0}^{N} \beta_n^{(L)} T_n(x) \quad \text{and} \quad \Phi_R(x) = \sum_{n=0}^{N} \beta_n^{(R)} T_n(x), \tag{60}$$

the expansion coefficients β_n can be expressed in terms of the expansion coefficients α of ϕ by means of the matrices $\mathbf{S}_L$ and $\mathbf{S}_R$, described near Eq. (48),

$$\vec{\beta}^{(L)} = \mathbf{S}_L\vec{\alpha} \quad \text{and} \quad \vec{\beta}^{(R)} = \mathbf{S}_R\vec{\alpha}. \tag{61}$$

The matrices $\mathbf{C}$, $\mathbf{C}^{-1}$, $\mathbf{S}_L$, and $\mathbf{S}_R$ can either be obtained from Ref. 4 or Ref. 11. We use Eqs. (58) and (61) to write the Chebyshev expansion of both sides of Eq. (52) as

$$\frac{1}{\Lambda}\vec{a} = \mathbf{M}_{\text{IEM}}\vec{a}, \tag{62}$$

where

$$\mathbf{M}_{\text{IEM}} = \frac{1}{2}\mathbf{C}^{-1}\mathbf{M}_3\mathbf{D}_{\mathcal{R}}\mathbf{C}. \tag{63}$$

The factor of 1/2 in Eq. (63) comes from the transformation of coordinates from r to x. The term L is canceled by the $(1/L)$ term in Eq. (54). $\mathbf{D}_{\mathcal{R}}$ is the diagonal matrix that contains the values of $\mathcal{R}(\xi_i)$ along the main diagonal, and $\mathbf{M}_3$ is given by

$$\mathbf{M}_3 = \mathbf{D}_G\mathbf{C}S_L\mathbf{C}^{-1}\mathbf{D}_F + \mathbf{D}_F\mathbf{C}S_R\mathbf{C}^{-1}\mathbf{D}_G. \tag{64}$$

The first (second) term in Eq. (64) represents the first (second) term in Eq. (54), $\mathbf{D}_F=\text{diag}(F)$ and $\mathbf{D}_G=\text{diag}(G)$ represent the diagonal matrices having the values of $F(\xi_i)$ and $G(\xi_i)$ along the main diagonal, and the ξ_i are the $N+1$ support points described near Eq. (39).

The explanation for Eq. (62) is as follows. The matrix $\mathbf{M}_{\text{IEM}}$ in Eq. (63) is applied to the column vector $\vec{a}$, the $\mathbf{C}$ in

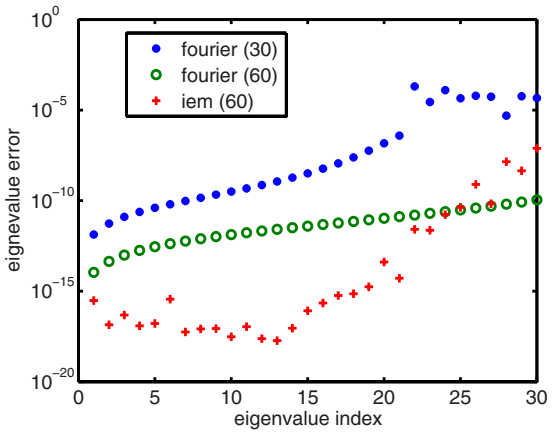

Fig. 10. Accuracy of the eigenvalues of $\mathbf{M}_{\text{fourier}}$ and $\mathbf{M}_{\text{IEM}}$ for various values of their dimension $N\times N$. The value of N is indicated in parenthesis in the legend. For the Fourier method, N is the number of basis functions ϕ_ℓ used to expand the Sturm–Liuoville eigenfunctions. For the integral equation, method N is the number of Chebyshev polynomials used in the expansion, which is also equal to the number of support points in the interval $[0,L]$. The accuracy of the matrix eigenvalues is obtained by comparison with Hartee's iterative method, which is accurate to one part in 10^{11} for all eigenvalue indices.

Eq. (63) transforms the $\vec{a}$ into the vector $\vec{\psi}$, and the factor $\mathbf{D}_{\mathcal{R}}$ together with the factor $\mathbf{D}_G$ in Eq. (64) transforms $\vec{\psi}$ into $\vec{G}\otimes\vec{\mathcal{R}}\otimes\vec{\psi}$. (The symbol $\otimes$ means that in $\vec{G}\otimes\vec{\mathcal{R}}$ each element of the vector $\vec{G}$ is multiplied by the corresponding element of the vector $\vec{\mathcal{R}}$, and a new vector of the same length is produced.) The additional factor $\mathbf{C}^{-1}$ produces the expansion coefficients of $\vec{G}\otimes\vec{\mathcal{R}}\otimes\vec{\psi}$, and the matrix S_L or S_R transforms these expansion coefficients to the expansion coefficients of the respective indefinite integrals. Equations (60)–(64) represent the IEM for evaluating an integral equation.

After choosing a value for the number $N_{\text{IEM}}+1$ of Chebyshev coefficients, a numerical value of the $(N_{\text{IEM}}+1)\times(N_{\text{IEM}}+1)$ matrix (63) is obtained, for which the eigenvalues $(1/\Lambda_n)$, $n=1,2,\ldots,N_{\text{IEM}}+1$ are calculated. The computing times for the Fourier method for both $N_{\text{fourier}}=30$ and 60 using the analytic expressions for the integrals needed to obtain the elements of the matrix $\mathbf{R}$ is 0.91 s (on a personal computer running Windows 7, using an Intel core TM 2 Quad, CPU Q 9950, running at 2.83 GHz, with 8.0 GB of RAM). By comparison, the combined computing time for the IEM for $N_{\text{IEM}}=30$, 60, and 90 is 0.75 s. We conclude that the integral equation method is comparable to or faster in speed than the Fourier expansion method, even if the overlap integrals (19) for the Fourier expansion method are known analytically. A disadvantage of the integral equation method for this application is that some eigenvalues are spurious. The occurrence of spurious eigenvalues can be recognized because they depend on the value of N_{IEM}, and are not close to any of the eigenvalues of $\mathbf{M}_{\text{fourier}}$.

The accuracy of the integral equation and the Fourier matrix methods, discussed in this section and in Sec. II B, respectively, is illustrated in Fig. 10. The accuracy test is based on a benchmark iterative method described in Sec. V, which gives an accuracy of one part in 10^{11} for each of the eigenvalues, regardless of the value of the eigenvalue index n. Figure 10 shows that the accuracy of the integral equation matrix method is considerably greater than the Fourier matrix method for low values of n. Figure 10 also shows that the accuracy of both matrix methods depends sensitively on the dimension N of their respective matrices $\mathbf{M}$.

V. THE ITERATIVE METHOD

The iterative method was introduced by Hartree[7] in the 1950s to calculate energy eigenvalues of the Schrödinger equation for atomic systems. The method was adapted to the use of the integral method 1 because of its predictable and high accuracy, and applied to the energy eigenvalue of the tenuously bound Helium-Helium dimer.[8] The version we will describe for finding the eigenvalues Λ_n that multiply the inhomogeneity function $\mathcal{R}$ is also suitable for finding the eigenfunctions of more general Sturm–Liouville equations, such as the Schrödinger equation.[21]

For a slightly incorrect value Λ_1 of Λ there is a slightly incorrect function ψ_1 that obeys the equation

$$\frac{d^2\psi_1(r)}{dr^2}+\Lambda_1\mathcal{R}(r)\psi_1(r)=0. \tag{65}$$

This function does not satisfy the boundary conditions at both $r=0$ and $r=L$, unless it has a discontinuity at some point r_I, in the interval $[0,L]$. The function ψ_1 to the left of r_I that vanishes at $r=0$ is denoted as $Y_1(r)$, and to the right of r_I the function that vanishes at $r=L$ is denoted as $kZ_1(r)$, where k is a normalization factor chosen such that $Y_1(r_I)=kZ_1(r_I)$. Both functions satisfy Eq. (65) in their respective intervals and are obtained by solving the integral equations

$$Y_1(r)=F(r)-\Lambda_1\int_0^{r_I}\mathcal{G}(r,r')\mathcal{R}(r')Y_1(r')dr',\quad (0\le r\le r_I), \tag{66}$$

and

$$Z_1(r)=G(r)-\Lambda_1\int_{r_I}^{L}\mathcal{G}(r,r')\mathcal{R}(r')Z_1(r')dr',\quad (r_I\le r\le L). \tag{67}$$

These integral equations differ from Eq. (52) due to the presence of the driving term F or G, defined near Eq. (54). Because the second derivatives of the latter functions are zero, their presence does not prevent Y_1 and Z_1 from satisfying Eq. (65) in their respective domains.

The iteration from Λ_1 to a value closer to the true Λ proceeds as follows. We multiply Eq. (68)

$$\frac{d^2Y_1(r)}{dr^2}+\Lambda_1\mathcal{R}(r)Y_1(r)=0\quad (0\le r\le r_I), \tag{68}$$

by $\psi(r)$ and multiply Eq. (4) by $Y_1(r)$. We then subtract one from the other, integrate from $r=0$ to $r=r_I$ and find

$$\int_0^{r_I}(Y_1''\psi-\psi''Y_1)dr'$$

$$=(Y_1'\psi-\psi'Y_1)_{r_I}=(\Lambda-\Lambda_1)\int_0^{r_I}Y_1\psi dr'. \tag{69}$$

Here a prime denotes the derivative with respect to r. A similar procedure applied to Z_1 in the interval $[r_I,L]$ yields

$$-k(Z_1'\psi-\psi' Z_1)_{r_I}=(\Lambda-\Lambda_1)\int_0^{r_I} kZ_1\psi dr'. \tag{70}$$

If we add these two results and remember that $kZ_1=Y_1$ for $r=r_I$, and divide the result by $\psi(r_I)kZ_1(r_I)$, we obtain

$$\Lambda-\Lambda_1=\frac{(Y'/Y-Z'/Z)_{r_I}}{\dfrac{1}{(Y_1\psi)_{r_I}}\displaystyle\int_0^{r_I} Y_1\mathcal{R}\psi dr'+\frac{1}{(Z_1\psi)_{r_I}}\int_{r_I}^{L} Z_1\mathcal{R}\psi dr'}. \tag{71}$$

Equation (71) is still exact, but the exact function ψ is unknown. The iterative approximation consists of replacing ψ in the first integral in the denominator by Y_1, and by kZ_1 in the second integral, and of replacing $\psi(r_I)$ in the denominators of each integral by either $Y_1(r_I)$ or by $kZ_1(r_I)$. The result is

$$\Lambda_2=\Lambda_1+\frac{(Y'/Y-Z'/Z)_{r_I}}{\displaystyle\int_0^{r_I} Y_1^2\mathcal{R}dr'/Y_1^2(r_I)+\int_{r_i}^{L} Z_1^2\mathcal{R}dr'/Z_1^2(r_I)}. \tag{72}$$

In Eq. (72) Λ was replaced by Λ_2 because it is a better approximation to Λ than Λ_1, and the normalization factor k has canceled out. The iteration proceeds by replacing Λ_1 in Eqs. (65)–(72) by the new value Λ_2, and by repeating the process until the change in Λ is less than a pre-determined value.

The derivatives in the numerator of Eq. (72) can be obtained without loss of accuracy by making use of the derivatives of Eqs. (66) and (67):

$$Y_1'(r)=F'(r)+\frac{\Lambda_1}{L}G'(r)\int_0^{r} F(r')\mathcal{R}(r')Y_1(r')dr'+\frac{\Lambda_1}{L}F'(r)\int_r^{r_I} G(r')\mathcal{R}(r')Y_1(r')dr', \tag{73}$$

and

$$Z_1'(r)=G'(r)+\frac{\Lambda_1}{L}G'(r)\int_{r_I}^{r} F(r')\mathcal{R}(r')Z_1(r')dr'+\frac{\Lambda_1}{L}F'(r)\int_r^{L} G(r')\mathcal{R}(r')Z_1(r')dr', \tag{74}$$

with the results at $r=r_I$

$$Y_1'(r_I)=1-\frac{\Lambda_1}{L}\int_0^{r_I} r'\mathcal{R}(r')Y_1(r')dr', \tag{75}$$

and

$$Z_1'(r_I)=-1+\frac{\Lambda_1}{L}\int_{r_I}^{L}(L-r')\mathcal{R}(r')Z_1(r')dr'. \tag{76}$$

The dimensions of Λ are ℓ^{-2}, and the dimension of F, G, Y, and Z are ℓ, where ℓ represents a unit of length. As noted, the derivatives with respect to r of the functions Y and Z are not obtained as the difference between two adjoining positions, but rather as the known derivatives of F and G, together with integrals (73) and (74) over Y and Z. In the integral equation formulation these integrals can be obtained with the same precision as the calculation of Y, Z, or ψ.[5] Hence there is no loss of accuracy for either the evaluation of Eq. (72) or for the calculation of Λ, which can be set to one part in 10^{11}. However, it is important to start the iterations with a value of Λ that lies within the range of convergence of Eq. (72). These initial values can be obtained, for example, from the eigenvalues of the matrix $\mathbf{M}_{\text{fourier}}$ or from the method described in Ref. 8.

Table III. Eigenvalues of Eq. (4) obtained iteratively using Eq. (72), for the purpose of providing benchmark values.

n	Λ_n	n	Λ_n
1	$1.61477559021\times10^{-1}$	26	$2.42220326385\times10^{-4}$
2	$4.06257259855\times10^{-2}$	27	$2.24611142229\times10^{-4}$
3	$1.81281029690\times10^{-2}$	28	$2.08854647313\times10^{-4}$
4	$1.02131986136\times10^{-2}$	29	$1.94699775697\times10^{-4}$
5	$6.54130338213\times10^{-3}$	30	$1.81936592475\times10^{-4}$

Some of the values for Λ_n found using the iterative method are listed in Table III. The initial values Λ_1 for each n are the results of the Fourier method with $N=60$. The iterations were stopped when the change $\Lambda_2-\Lambda_1$ became less than 10^{-12} (usually three iterations were required), and tol $=10^{-11}$.

The error of the functions Y and Z is given, according to Eq. (42), by the size of the high order Chebyshev expansion parameters. For tol$=10^{-11}$ their values are less than 10^{-11}, as is shown in Fig. 11. Because there is no loss of accuracy in evaluating the various terms in Eq. (72), the error in the iterated eigenvalues Λ is also given by Fig. 11. To achieve this accuracy, the number N of Chebyshev polynomials used for the spectral expansion of the functions Y and Z for the solution of their respective integral equations was increased adaptively. It was found that for $n=1$, $N=16$; for $n=2-6$, $N=24$; for $n=7-23$, $N=24$; and for $n=18-30$, $N=54$. This procedure of increasing N is different from the procedure used in Ref. 8, where N was kept constant and the number

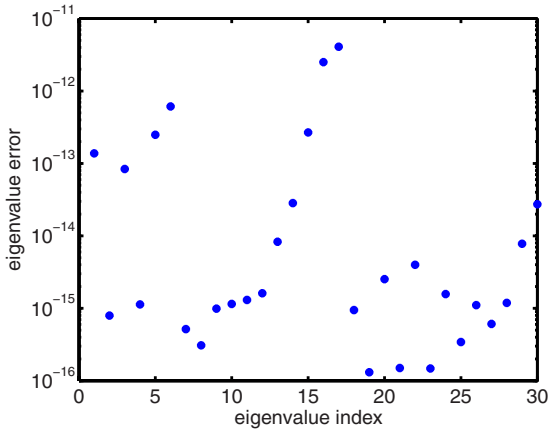

Fig. 11. The absolute value of the mean square average of the three last Chebyshev coefficents in the expansions of the functions Y and Z. As discussed in the text, the error of the eigenvalues Λ is also given by the y-axis. The number N of expansion Chebyshev polynomials was increased adaptively as the eigenvalue index n increased. The "jumps" in the values of these errors is due to the transition from one value of N to a larger value. The figure demonstrates that all inaccuracies stay below one part in 10^{11}, in agreement with the accuracy parameter tol specified to be 10^{-11}.

and size of the partitions in the domain of r was increased adaptively. The latter method was required because of the long-range behavior of the He–He wave functions.

VI. SUMMARY AND CONCLUSIONS

The main goal of this paper is to describe the Chebyshev expansion method for solving integral equations, with the hope that this method will be included in computational physics courses. This expansion method converges rapidly (spectrally) and complements the usual finite difference methods. The example used for the application of this method is the vibration of an inhomogeneous string in the separation of variables formalism. The basis functions $\psi_n(r)$, $n=1,2,\ldots$, form a complete Sturm–Liouville set, the calculation of which is performed by three methods. In the Fourier expansion method the function ψ is expanded into a basis set of sine waves, and the eigenfrequencies and expansion coefficients for each ψ_n are the eigenvalues and eigenvectors of the matrix $\mathbf{M}_{\text{fourier}}$. In the integral equation method the differential equation for ψ_n is transformed into an integral equation of the Lippmann–Schwinger type, the unknown function is expanded into Chebyshev polynomials, and the expansion coefficients are the eigenvectors of a matrix $\mathbf{M}_{\text{IEM}}$. The comparison of these two methods illustrates the differences and advantages of each, especially their properties as a function of the size of the expansion basis. In the third method (the extended Hartree method) the differential equation for the Sturm–Liouville eigenfunction is solved iteratively. This hybrid method combines Hartree's iterative method of finding eigenvalues of a differential equation with the highly accurate integral equation method for providing the auxiliary functions needed to implement the iterations. The advantage of this hybrid method is that the precision of both the eigenfunction and the eigenvalue can be pre-determined, and no eigenvalue calculation of big matrices is required. In the present application the results of this method were accurate to one part in 10^{11}. Applications of these methods to other problems, such as the solution of the Schrödinger equation, or the heat propagation equation, or diffusion equations in biology are possible.

[1] C. F. Gerald and P. O. Wheatley, *Applied Numerical Analysis*, 6th ed. (Addison-Wesley, Reading, MA, 1999); S. Koonin, *Computational Physics* (Benjamin-Cummings, New York, 1985); Rubin H. Landau and M. J. P. Mejía, *Computational Physics: Problem Solving with Computers* (John Wiley & Sons, New York, 1997); Paul L. DeVries and Javier E. Hasbun, *A First Course in Computational Physics*, 2nd ed. (Jones and Bartlett, Sudbury, MA, 2010).

[2] R. Chabay and B. Sherwood, "Computational physics in the introductory calculus-based course," Am. J. Phys. **76**, 307–313 (2008); D. M. Cook, "Computation in undergraduate physics: The Lawrence approach," *ibid.* **76**, 321–326 (2008); C. Rebbi, "A project-oriented course in computational physics: Algorithms, parallel computing, and graphics," *ibid.* **76**, 314–320 (2008); Harvey Gould, "Computational physics and the undergraduate curriculum," Comput. Phys. Commun. **127**, 6–10 (2000).

[3] G. Rawitscher, I. Koltracht, H. Dai, and C. Ribetti, "The vibrating string: A fertile topic for teaching scientific computing," Comput. Phys. **10**, 335–340 (1996).

[4] R. A. Gonzales, J. Eisert, I. Koltracht, M. Neumann, and G. Rawitscher, "Integral equation method for the continuous spectrum radial Schrödinger equation," J. Comput. Phys. **134**, 134–149 (1997); R. A. Gonzales, S.-Y. Kang, I. Koltracht, and G. Rawitscher, "Integral equation method for coupled Schrödinger equations," *ibid.* **153**, 160–202 (1999).

[5] G. Rawitscher and I. Koltracht, "Description of an efficient numerical spectral method for solving the Schrödinger equation," Comput. Sci. Eng. **7**, 58–66 (2005); G. Rawitscher, in *Operator Theory, Advances and Applications*, edited by Thomas Hempfling (Birkäuser Verlag, Basel, 2009), Vol. 203, pp. 409–426.

[6] A. Palacios, T. N. A. Rescigno, and C. W. McCurdy, "Two-electron time-delay interference in atomic double ionization by attosecond pulses," Phys. Rev. Lett. **103**, 253001 (2009); W. Glöckle and G. Rawitscher, "Scheme for an accurate solution of Faddeev integral equations in configuration space," Nucl. Phys. A. **790**, 282c–285c (2007).

[7] D. R. Hartree, *The Calculation of Atomic Structures* (John Wiley & Sons, New York, 1955), p. 86.

[8] G. Rawitscher and I. Koltracht, "An economical method to calculate eigenvalues of the Schrödinger equation," Eur. J. Phys. **27**, 1179–1192 (2006).

[9] Lloyd N. Trefethen, *Spectral Methods in Matlab* (SIAM, Philadelphia, PA, 2000); John P. Boyd, *Chebyshev and Fourier Spectral Methods*, 2nd revised ed. (Dover Publications, Mineola, NY, 2001).

[10] G. W. Recktenwald, *Numerical Methods with Matlab: Implementation and Application* (Prentice Hall, Upper Saddle River, NJ, 2000).

[11] ComPADRE is a digital library located at ⟨www.compadre.org/ucomp⟩.

[12] L. P. Fulcher, "Study of the eigenvalues of a nonuniform string," Am. J. Phys. **53**, 730–735 (1985); H. P. W. Gottlieb, "Isospectral strings," Inverse Probl. **18**, 971–978 (2002); P. Amore, "The string of variable density: Perturbative and non-perturbative results," Ann. Phys. **325**, 2679–2696 (2010).

[13] C. O. Horgan and A. M. Chan, "Vibration of inhomogeneous strings, rods and membranes," J. Sound Vib. **225** (3), 503–513 (1999).

[14] Mary L. Boas, *Mathematical Methods in the Physical Sciences*, 2nd ed. (John Wiley & Sons, New York, 1983), Prob. 24, p. 540; D. A. McQuarrie, *Mathematical Methods for Scientists and Engineers* (University Science Books, Sausalito, CA, 2003), p. 687.

[15] C. W. Clenshaw and A. R. Curtis, "A method for numerical integration on an automatic computer," Numer. Math. **2**, 197–205 (1960).

[16] T. J. Rudin, *The Chebyshev Polynomials* (John Wiley & Sons, New York, 1974).

[17] Y. L. Luke, *Mathematical Functions and Their Approximations* (Academic Press, New York, 1975), Sec. 11.7.

[18] A. Deloff, "Semi-spectral Chebyshev method in quantum mechanics," Ann. Phys. (N.Y.) **322**, 1373–1419 (2007).

[19] D. Gottlieb and S. A. Orszag, *Numerical Analysis of Spectral Methods: Theory and Applications*, CBMS-NSF Regional Conference Series in Applied Mathematics Vol. 26 (SIAM, Philadelphia, 1977).

[20] A. Deloff, "Gauss-Legendre and Chebyshev quadratures for singular integrals," Comput. Phys. Commun. **179**, 908–914 (2008).

[21] G. Rawitscher, "Positive energy Weinberg states for the solution of scattering problems," Phys. Rev. C **25**, 2196–2213 (1982).